Materials Physics and Mechanics 25 (2016) 16-21 Received: October 15, 2015

DISSIPATION OF ENERGY AND INSTABILITY PROCESS IN VARIOUS ALLOYS BASED ON PLASTOMETRIC TESTS

J. Klíber

VŠB-TU Ostrava, FMMI, Department of Materials Forming, 17.listopadu 15, 708 33,

Ostrava–Poruba, Czech. Republic

e-mail: jiri.kliber@vsb.cz

Abstract. Energy dissipation and plastic flow instability were investigated in P91 steel and Ms70 brass on the basis of continuous tests carried out on Setaram and Gleeble plastometers. Mathematical evaluation of continuous curves was supported with calculation of larger range of input parameters using the "sin h" equation. For energy dissipation calculation strain rate sensitivity parameter (m=(d lnσ)/(d lnė)) was computed and further the efficiency according to the η=2m/(m+1) formula. Equation ξ=(∂ ln(m/(m+1)))/(∂ lnė)+m was utilized for the instability parameter calculation. The results were evaluated using Sigmacon, Gnuplot and Golden Surfer computer softwares. The final results are 2D and 3D material processing maps. Results of tests carried out with P91 steel and Ms70 brass were compared to experimental results of other authors with high correlation.

1. Introduction

Material machinability and formability depends on its ability to deform plastically during forming process without its rupture. The work [1] presents a finding of the authors Prasad and Sasidhara who deal with process maps that formability consists of two independent components: internal formability, which is influenced by evolution of microstructure at specific conditions of the given process, and external formability, which is influenced by geometry of the deformation zone and stress conditions at forming [2-4]. These maps are used at forming of steel, as well as of alloys made of non-ferrous metals (aluminium, magnesium, nickel, titanium alloys, etc.). Forming of some alloys may be very difficult and process maps make it possible to suggest the best possible solution of method for their processing [5-7].

2. Power dissipation, process maps

Power dissipation at forming is characterised by dimensionless variable, power dissipation efficiency η. It is used as a crucial element by one of the most widespread models, dynamic material model (DMM – Dynamic Material Modelling) [8]. The dependence of stress on the strain rate at given temperature is determined by the curve and the dependence of sensitivity of plastic flow to the strain rate is expressed as a function of strain rate [9]. The process map thus represents the areas, at which it is appropriate to form the material, and on the other hand the areas, in which forming can become already dangerous for the given material. Maps of power dissipation are expressed in coordinates of deformation temperature and strain rate logarithm. Forming is in this interpretation considered to be a power system, where power is dissipated in the deformation zone [10, 11].Total power absorbed by the body during deformation (P) consists in principle of two components at I may be expressed by the following equation:

$$P = G + J, \tag{1}$$

where P – total power absorbed by the body during deformation [J], G – power dissipated in consequence of plastic deformation [J], J – power dissipated in consequence of microstructural changes [J].

Distribution of total power between power components J and G is described by the coefficient of sensitivity of the material plastic flow to the strain rate [1]. Knowledge of this coefficient is indispensable for creation of process map; it can be expressed in the following manner:

$$m = \frac{dJ}{dG} = \frac{\dot{e} \cdot d\sigma}{\sigma \cdot d\dot{e}} = \frac{d \ln \sigma}{d \ln \dot{e}}. \tag{2}$$

Coefficient m is function of the strain rate.

For creation of process map, it is highly necessary to know also a dimensionless parameter η, i.e. efficiency of power dissipation. The following formula is valid for the parameter η:

$$\eta = \frac{J}{J_{\max}} = \frac{2m}{m+1}. \tag{3}$$

The results are multiplied by one hundred to obtain percentage values, which is usual way of expressing the efficiency. The parameter of plastic instability is also of no less importance, as it makes it possible to determine, in which areas the material deformation is stable, and in which areas material rupture may occur already during forming [12-15]. Parameter of plastic instability can be calculated by this formula:

$$\zeta = \frac{\partial \ln\left(\frac{m}{m+1}\right)}{\partial \ln \dot{e}} + m, \tag{4}$$

where ξ – parameter of plastic instability, m – strain rate sensitivity, $\dot{e}$ – strain rate [s^{-1}].

3. Experiment torsion test

Continuous test to rupture is the most frequently performed test on the plastometer SETARAM. Determination of the stress-strain curve is made by comparatively complicated calculation method [16]. Torsion tests were performed on various materials – steel and brass. In case of the steel P91 the samples were investigated at the temperatures ranging from 1223 K to 1473 K and at strain rates ranging from 0.0965 to 1,53 s^{-1} [17].

Hot torsion tests of brass Ms70 (Cu + 30 wt.% Zn) were performed at 4 strain rates, namely 0.2; 1; 5; and 10 s^{-1}, corresponding to torsion revolutions 16; 80; 400 and 800 rpm, and at five temperature levels t= 923, 973, 1023, 1073 and 1123 K [18].

4. Experiment compression test

Plane strain compression test was performed on the plastometer Gleeble 3800.

Altogether 12 tests were made at 3 strain rates $\dot{e}$ = 0.1; 1 and 10 s^{-1}, and at temperatures ranging from 800 °C to 1260 °C on the material 9Cr (P91). For extrapolation of the courses also for lower and higher strain rates than the tested one, the activation power Q was calculated and afterwards the value of stress was determined from it by the following equation.

$$\sigma = \frac{1}{\alpha} \exp\left(\arg\sinh\left[\frac{\dot{e} \exp\left(\frac{Q}{RT}\right)}{A} \right]^{\frac{1}{n}} \right). \tag{5}$$

5. Results and evaluation of the brass Ms70

Figure 1 shows the dissipation map for the magnitude of deformation of 0.5 brass with 30 % Zn. The map was calculated from the values published in [19, 20]. If we compare it directly with the map from the work, we may notice certain differences. First of all the area of high temperatures and low strain rates is different. In the original map the dissipation increases in this area. However, in the map re-calculated by us an area appears with a decrease and subsequent increase. This may be attributed to the algorithm of formation of a spatial map, when the method used by us prevents an excessive smoothing of curves of the dissipation coefficient, processed for individual temperature levels. The map of power dissipation from the data taken from [19] was constructed for verification of the whole calculation procedure, as well as for its direct comparison with the map of power dissipation at the torsion test (the map plotted by dashed lines in Fig. 1). The range of strain rates and deformation temperatures is limited in comparison with the published results. The area of higher strain rates cannot be covered by the torsion plastometer SETRAM due to physical limitations of the torsion test [16]. Lower strain rates are achievable with use of additional gearbox.

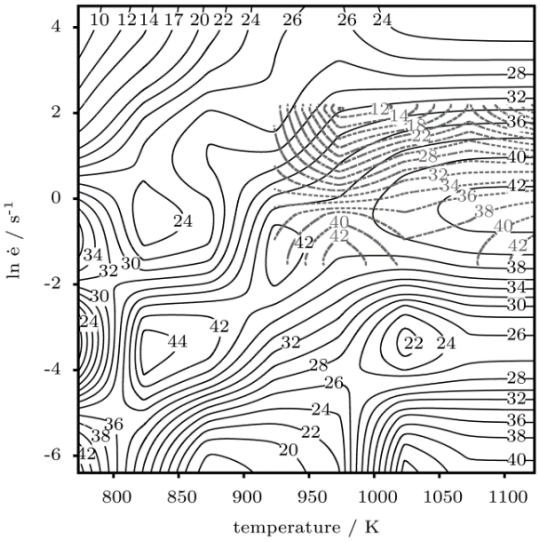

Fig. 1. Superposition of the maps of power dissipation of brass Ms70 for deformation of 0.5. Solid lines are plotted on the basis of data from literature [19] that were measured by compression plastometer; dashed lines were plotted on the basis of torsion tests.

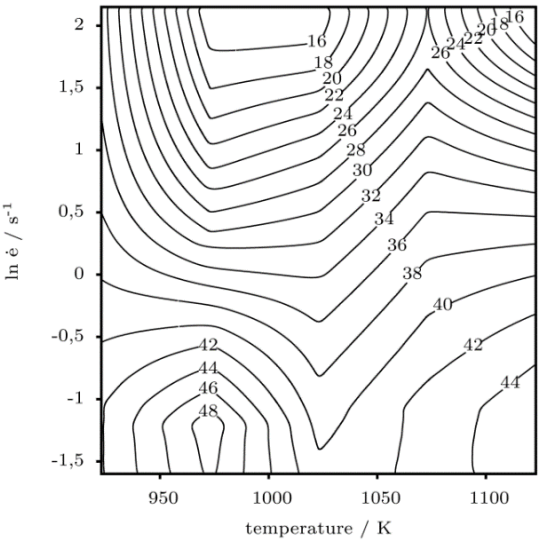

Fig. 2. Power dissipation [percentage] for brass Ms70 at the deformation of 0.9.

They were, however, not realised due to orientation of the original experiment on the area of occurrence of dynamic recrystallization as the controlling softening process. If we compare the shape with the adapted dissipation map, we can see its conformity with the shape for brass with 30 % of Zn. It is, nevertheless, necessary to admit that point of the limit strain rates were significantly influenced, since determination of the parameter miss highly sensitive to the algorithm used for calculation of cubic splines and for exact determination of the value of resistances to deformation. They were then used for calculation of the strain rate sensitivity coefficient *m*.

Advantage of the torsion test consists on realisation of big deformations, which cannot be made on compression plastometers. It was thus possible to construct the dissipation maps also for bigger values of deformation. Evaluation for the deformation of 0.9 in Fig. 2 may serve as an example. The final map shows higher efficiency of power dissipation into micro-structural state at lower strain rates – for all deformation temperatures [21].

6. Results and evaluation of the STEEL 9Cr

The principles of Dynamic Material Modelling were used for construction of maps of power dissipation.

The following steps were taken for obtaining of the coefficient of power dissipation η. The value of resistance to deformation for individual tested temperature levels and strain rates was read from the dependence of the deformation stress for a constant deformation (Fig. 3.).

Thus obtained dependences of stress-strain rate were recalculated to the dependence stress logarithm-strain rate logarithm. If we compare the course of the strain rate coefficient m on the logarithm of strain rate, the values are comparable for the steel 9Cr regardless of the type of testing machine. The course of mind is in dependence on the strain rate logarithm identical, only the values of both quantities differ. These calculations were finally performed for the deformations of 0.3; 0.5 and 0.9 in order to enable comparison with the same steel 9Cr, which was investigated on the plastometer Gleeble [22].

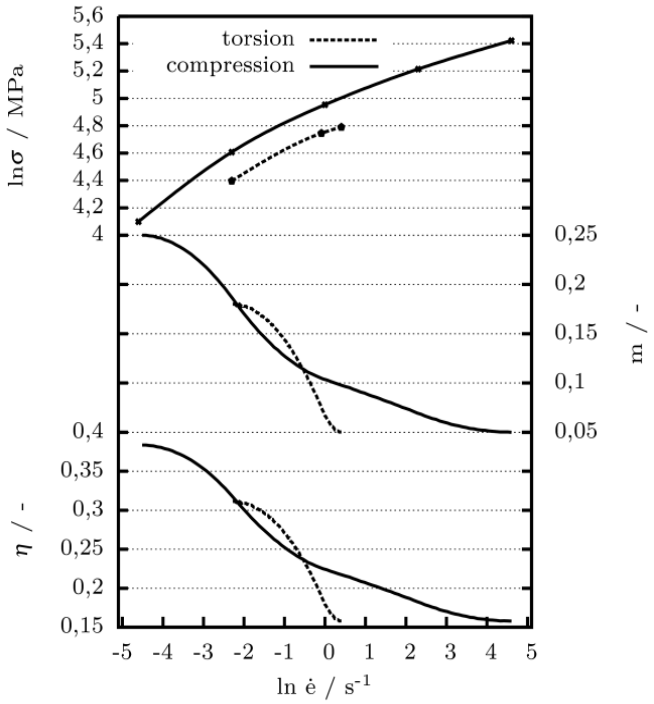

Fig. 3. Procedure used for processing of the results of plastometric tests for the temperature of 1050 °C from the stresses measured at the deformation of 0.5 to the coefficient of sensitivity to the strain rate *m* and efficiency of dissipation *η*.

Figure 4 represents an example of a 2D diagram of power dissipation, in this case for deformation e = 0.5 performed on the plastometer Gleeble. For comparison the same steel and the same deformation was analysed with use of the torsion plastometer SETARAM (Fig. 5). Nevertheless, at evaluation a magnification of the range of strain rates by the formula (5) was not used and instead directly determined values of stress were used for calculation of dissipation efficiency.

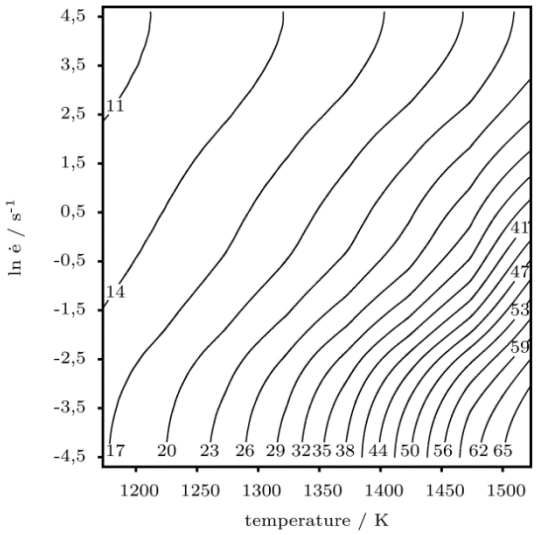

Fig. 4. Power dissipation [percentage] for 9 Cr at the deformation of 0.5 on the basis of compression tests.

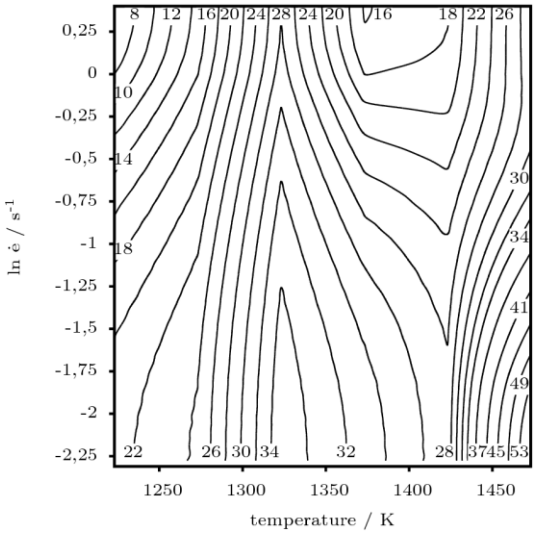

Fig. 5. Power dissipation [percentage] for 9 Cr at the deformation of 0.5 on the basis of torsion tests.

7. Conclusions

Procedure of evaluation of results of plastometric tests was first tested on data from literature for the brass with 30 % of Zn. The map of power dissipation created on the basis of results measured by the plastometer SETARAM was compared with the already published map. Very good agreement was obtained in the area of lower strain rates. In case of the steel 9Cr we have compared the results obtained on the plastometers Gleeble and SETARAM. Different chosen procedures led to somewhat different results of the course of power dissipation. It appears from the images of the process maps for the steel 9Cr that forming in the area below approx. 975 °C

and at higher strain rates is unsuitable, and that the temperature range between 1050 °C and 1100 °C is also less suitable.

We assume that we will be able to determine the dissipation by this method at analyses of data obtained also from other materials, as well as another parameter ξ, which are the possible areas of deformation instability.

Acknowledgements

This paper was created on the Faculty of Metallurgy and Materials Engineering in the Project No. LO1203 "Regional Materials Science and Technology Centre – Feasibility Program" funded by Ministry of Education, Youth and Sports of the Czech Republic.

References

[1] Y.V.R.K. Prasad, K.P. Rao // *Materials and Design* **30** (2009) 3723.
[2] Y.V.R.K. Prasad, K.P. Rao // *Materials Science and Engineering* A **487** (2008) 316.
[3] Juan Liu, Zhenshan Cui, Congxin Li // *Journal of Materials Processing Technology* **205** (2008) 497.
[4] J. Petruželka, P. Sonnek, *Analýza procesu tváření za tepla: Dynamický materiálový model* (VŠB-TU Ostrava: Ostrava, 2001).
[5] J. Kliber, In: *Sborník vědeckých prací Vysoké školy báňské* (Technické univerzity Ostrava, řada hutnická, 2009), LII (3), p.95.
[6] J. Kliber, In: *Proceeding of the Forming 97* (Austria, Salzburg, June 5-9, 2011), p. 61.
[7] J. Kliber, In: *Proceeding of the Conference "Machine-Building and Techno sphere at the Boundary of the XXI Century" (*Doneck, 2001), p.144.
[8] Guoliang Ji, Fuguo Li, Qinghua Li, Huiqu Li, Zhi Li // *Materials Science and Engineering A* **527** (2010) 1165.
[9] Guo-zheng Quan, Lei Zhao, Tao Chen, Yang Wang, Yuan-ping Mao, Wen-quan Lv, Jie Zhou // *Materials Science and Engineering A* **538** (2012) 364.
[10] H. Li, M.Q. Li, X.Y. Zhang, J. Luo // *Materials Science and Engineering A* **527** (2010) 6505.
[11] H.J. McQueen, N. Jin, N.D. Ryan // *Materials Science and Engineering A* **190** (1995) 43.
[12] Yu Sun, Wei-dong Zeng, Yong-qing Zhao, Xue-min Zhang, Xiong Ma, Yuan-fei Han // *Transactions of Nonferrous Metals Society of China* **21** (2011) 159.
[13] J. Petruželka et.al. *Analýza procesu tváření za tepla. Integrovaný model* (VŠB-TU Ostrava: Ostrava, 2001).
[14] Yongquan Ning, Zekun Yao, Hongzhen Guo, M.W. Fu, Hui li, Xinghua Xie // *Material Science and Engineering A* **527** (2010) 6794.
[15] A. Momeni, K. Dehghani // *Materials Science and Engineering A* **528** (2011) 1448.
[16] I. Schindler, J. Boruta *Utilization Potentialities of the Torsion Plastometer* (Silesian Technical University Katowice: Katowice, 1998).
[17] L. Kunčická, In: *Master thesis, FMMI* (VŠB-Technical University Ostrava, 2012).
[18] T. Kubina, J. Bořuta, R. Pernis // *Materials and Technology* (in print).
[19] Y.V.R.K. Prasad, S. Sasidhara, *Hot Working Guide: Compendium of Processing Maps* (ASM International, 1997).
[20] D. Padmavardhani, Y.V.R.K. Prasad // *Metallurgical Transactions* A **22 (12)** (1991) 2985.
[21] T. Kubina, J. Kliber, L. Kunčická, In: *Proceeding of the 22nd International Conference on Metallurgy and Materials METAL2013* (Czech Republic, EU, Brno, May 15-17, 2013), p.456.
[22] M. Berková, In: *Master thesis, FMMI* (VŠB-Technical University Ostrava, 2012).